Modelling of Alternative Propulsion Concepts of Railway Vehicles

Holger Dittus Jörg Ungethüm
Deutsches Zentrum für Luft- und Raumfahrt
Pfaffenwaldring 38-40, 70569 Stuttgart
holger.dittus@dlr.de joerg.ungethuem@dlr.de

Abstract

Hybrid power trains as increasingly used in road vehicles become more and more interesting for railroad vehicles. Short-distance passenger traffic on non-electrified lines is a domain where brake energy recuperation might reduce the total energy consumption significantly. In this paper a simulation model of a light diesel-powered railcar is presented. Model components are adapted from standard Modelica and Powertrain library. The potential improvement of fuel economy regarding different application settings is evaluated.

Keywords: model, simulation, railroad, power train, hybrid, energy consumption, drive strategy

1 Introduction

In contrast to road vehicles there were no compulsory emission limits for railroad vehicles in the past. In the domain of diesel driven railway vehicles there is only a voluntary emission limitation for nitric oxide and particles by the International Union of Railway (UIC), which is obligatory for its members. With the beginning of the year 2006 new tightened up restrictions by the European Union for new and repowered railcars take effect. Further decrease of emissions is settled for the year 2012. In this context effort is also spent on increasing the fuel efficiency of railcars.

In this work a model for dynamic simulation of diesel driven railroad vehicles is developed. This contains models for driving resistance, longitudinal section of the track, combustion engine, electric motor and generator, as well as gearboxes. Energy storages like flywheels and ultracapacitors are implemented for the simulation of hybrid vehicles.

The component models are combined to exemplary railcar power train configurations for local and regional traffic. The effect of different power train configurations and different driving strategies is demonstrated. Pure electric vehicles are not in the scope of this work. However, the electric components might also be used to model those vehicles.

2 State of the Art

2.1 Railway vehicle power trains

In diesel railcars and locomotives hydromechanic or electric power transmissions are used. For light railcars most often the hydromechanic power transmission is used. The automatic transmission and the diesel engine are frequently adapted from road vehicle mass products. The electric power transmission consists of the diesel engine, which is rigidly coupled with an electric generator, and the electric traction motors. It is most often used in high speed railcars and heavy diesel locomotives. However, the electric power train can easily be transformed into a serial hybrid power train by adding an electric storage which makes it attractive even for short-distance railcars.

2.2 Comparison of commercial and rail vehicles

In commercial and public transport vehicles hybrid power trains are primarily used in two different applications. A significant number of busses for local urban traffic and light delivery vans, used in post and express service, are featured with alternative or hybrid power trains, predominantly in the USA. In most cases, serial or power split hybrid power trains are in use. In some cases also fuel cells or battery powered electric drives are in trial and in regular use.

Up to now, hybrid power trains in railroad vehicles are rare. However, some railroad manufacturer conducted experiments to use energy storages in railroad vehicles for braking energy recuperation. A current mass product is the “GreenGoat” which is a diesel-electric shunt locomotive built by the Canadian manufacturer Railpower Technology Corp. This lo-

comotive has a traction power of 2000kW and is featured with a 1200Ah lead battery.

Electric brakes for electric and diesel-electric railroad vehicles are well known. Braking energy is either converted into heat by brake resistors or it is fed back into the contact wire. Electric brakes are used as service brake because they are wear-free and non-exhaustible.

In the domain of short-distance passenger traffic on non-electrified lines light railcars with a tare weight between 23t (e.g. DWA LVT/S) and 120t (e.g. ALSTOM Corodia LIREX) are in use. A typical example is the RegioShuttle RS1 (former Adtranz, now Stadler) which has a maximum total weight of 56t. This railcar is the most commonly used diesel powered railcar in Germany. The power train of this railcar is based on a conventional road bus power train.

2.3 Driving cycles and driving styles

In a typical driving cycle a railroad vehicle is accelerated with the maximum tractive force up to the admissible maximum speed (acceleration phase). This speed is kept until short before the next halt (constant speed phase), where the vehicle is braked with the maximum service deceleration (deceleration phase). Changes of the admissible maximum speed are also realized with maximum acceleration or deceleration. This driving style leads to the shortest possible travelling time which is possible for a given vehicle.

The ”energy saving” driving style uses the recovery margin of the timetable. The recovery margin is about 5 to 10% of the minimum travelling time and is considered in timetables to recover delays. It can be used to reduce the maximum speed or to join a roll out phase between constant speed and deceleration phase.

2.4 Driving strategies of serial hybrid power trains

The driving strategy of a serial hybrid power train determines how each component of the power train is driven. One category of driving strategies lets the power of the diesel engine follow the actual power of the electric traction motor. There is still a variation in the diesel engine rotating speed possible, which can be optimized to reduce total fuel consumption. In the classical diesel-electric power train without any energy storage this is the only possible driving strategy. Another category of driving strategies decouples the power of the diesel engine from the actual power of the traction motor. Obviously, an energy storage is required in this case. As the working conditions of the diesel engine can be shifted towards its optimum a lower fuel consumption can be expected.

2.5 Energy storages

Railroad vehicles are commonly built for a lifetime of 25 to 30 years. The time between two general overhauls is 8 to 10 years. The huge number of charge/discharge cycles within this period would lead to high battery masses to obtain sufficient battery life-time, which makes batteries not yet suitable for railcar hybrid power trains.

Flywheels are used in railroad applications as stationary energy storage to buffer peak loads of contact wires. As flywheels are proved to be usable in mobile applications, e.g. road busses, they can also be used in railroad vehicles. Flywheels are nowadays built from fibre composite which enables very high rotation speed and reduces the impact in case of burst. Flywheels are best for energy storage in the time-range of several minutes.

Ultracapacitors are known for high power density and huge number of charge/discharge cycles. They are already applied in railroad applications for brake energy recovery (Bombardier MITRAC Energy Safer).

3 Modelling of the components

3.1 Driving resistance

The driving resistance of a railroad vehicle consists of the rolling resistance, climbing resistance, drag resistance, curved track resistance, and acceleration resistance.

$$F_W = F_{Roll} + F_{Slope} + F_{Drag} + F_{Curve} + F_a$$

The rolling resistance of a railroad vehicle is small compared to road vehicles. It is calculated from the total weight of the vehicle using the rolling resistance coefficient.

$$F_{Roll} = m_{Vehicle} \cdot \vec{g} \cdot f_R \cdot \cos(\alpha_{Slope})$$

$$f_R = 0.0015 \ldots 0.0040$$

The climbing resistance is calculated from the mass of the vehicle and the ascent angle. For longer trains the mass of the train must be described as mass strap, where the ascent might vary between different parts of the train. In this work, only short railcars are considered, so the train is treated as a single mass point. It is common to specify the ascent in tenth of percent.

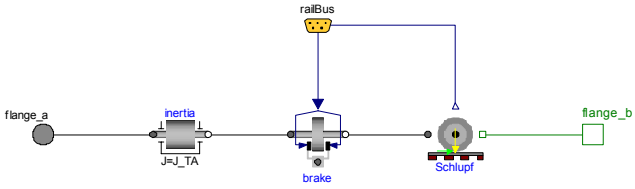

Figure 1: Model of the driven axle

$$F_{Slope} = m_{Vehicle} \cdot \vec{g} \cdot \sin(\alpha_{Slope}) = m_{Vehicle} \cdot \vec{g} \cdot \sin(\tan^{-1}(p))$$

The drag resistance is assumed to be proportional to the square of the driving velocity. For longer trains (esp. freight trains) the lateral air resistance of the wagons is dominant. For short railcars which are the focus of this work, the lateral air resistance is not calculated separately.

$$F_{Drag} = \frac{1}{2} \cdot \rho_{Air} \cdot c_W \cdot A \cdot v_{Vehicle}^2$$

The curved track rolling resistance is commonly calculated by an empiric formula. However, there are a number of different approaches. In this work, a simple formula, which is valid in average cases, is used:

$$F_{Curve} = \frac{0{,}75 \cdot m_{Vehicle} \cdot \vec{g}}{R_{Curve}}$$

The translatory acceleration resistance is calculated by Newton's law.

$$F_a = m_{Vehicle} \cdot a_{Vehicle}$$

The longitudinal section of the track including gradient, curvature data and admissible maximum speed is read from a data file.

3.2 Axles

The models of the axles are one of the main components. They are connected to the model of the chassis. There are models for driven and non-driven axles which are very similar. The models might be used for bogies, too. The model of the driven axle is shown in Figure 1. Its connectors are the abstractions of the driving shaft and the axle box which transmits the driving force to the model of the driving resistance. The component 'Schlupf' calculates friction and slip between the track and the wheel in the contact point. The actual slip is fed as input signal for the wheel sliding protection and the wheel skid protection.

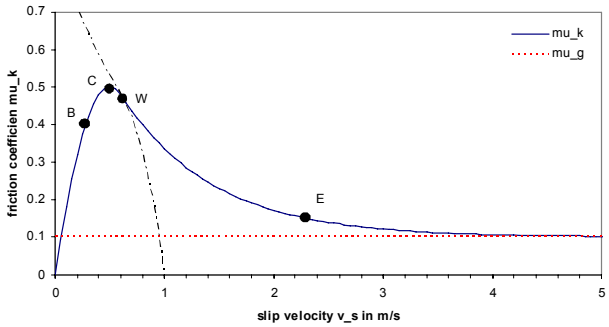

Figure 2: Approximation of friction coefficient as a function of slip velocity

3.3 Friction and slip between track and wheel

The small friction coefficient between track and steel wheel makes it necessary to calculate the slip, as acceleration and deceleration might be limited by the transmittable force in the contact point. Neglecting track gradient and vertical acceleration of the chassis, the perpendicular force is constant. The maximum friction coefficient is a function of vehicle speed and track condition. For the acceleration phase, the approach

$$\mu_{T,max} = k_1 + \frac{k_2}{k_3 + v_{Fzg}}$$

is commonly used. The values of the constants were empirically investigated by Curtius and Kniffler. Even though modern vehicles do achieve higher friction coefficients, these values are still used in vehicle design to ensure sufficient friction even under worse conditions.

k_1	k_2	k_3
0,161	2,083 m/s	12,222 m/s

The actual value of the friction coefficient is a function of the actual slip velocity.

$$v_{slip} = R_{wheel} \cdot \omega_{wheel} - v_{vehicle}$$

The function $\mu_K(v_{slip})$ is built from a combination of a 2nd order polynomial and an exponential function (Figure 2). This curve is an approximation of three different friction mechanisms. In the range 0 to B the so-called microslip dominates. The friction coefficient is nearly linear to the slip velocity. Between B and the maximum friction coefficient at C a rapid alternation of minimal slipping and sticking (slip-stick-movement) dominates. For higher values of

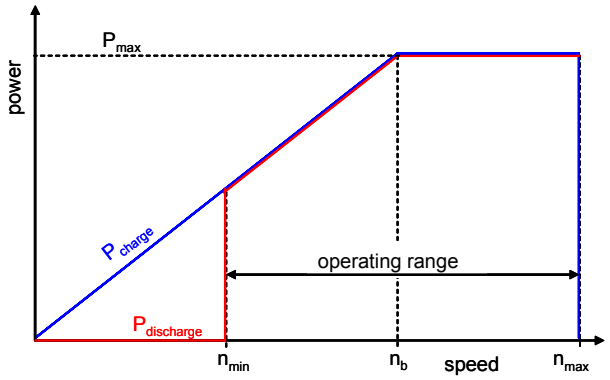

Figure 3: Flywheel operating characteristic

slip velocity, the friction coefficient decreases dramatically leading to a significant heating of the material in the contact point followed by further decrease of the friction coefficient. In most cases, measured values for μ_B and μ_W are not available. A reasonable approach is [1]:

$$\mu_K = \begin{cases} 2 \cdot \mu_C \cdot \frac{v_{slip}}{v_C} \cdot \left(1 - \frac{v_{slip}}{2 v_C}\right) & \forall \quad v_{slip} \le v_W \\ D \cdot \exp\left(-\omega \cdot v_{slip}\right) + \mu_\infty & \forall \quad v_{slip} > v_W \end{cases}$$

$$\omega = -\frac{T}{\mu_W - \mu_\infty} \qquad T = \frac{2 \cdot \mu_C}{v_C}\left(1 - \frac{v_W}{v_C}\right)$$

$$D = \left(\mu_W - \mu_\infty\right) \cdot \exp\left(-\omega \cdot v_W\right)$$

$$\alpha = \frac{\mu_W}{\mu_C} \approx 0.95$$

$$\mu_\infty \approx 0.1$$

As input for the wheel sliding and wheel skid protection a variable slip is defined as the ratio:

$$slip = \frac{v_{slip}}{v_C}$$

3.4 Wheel skid and wheel slide protection

In this model, the actual slip is available as input signal for the skid and slide protection. This enables the implementation of a perfect slip and slide protection. In reality, in most cases only the wheel rotating speed is available. However, the internals of the skid and slide protection are beyond the scope of this work. For the aim of energy consumption prediction the approach of a perfect controlled system is sufficient. The skid protection reduces the driving power if the slip exceeds 0.8 until zero at slip 1.0. The slide protection works analogue in reducing the brake force.

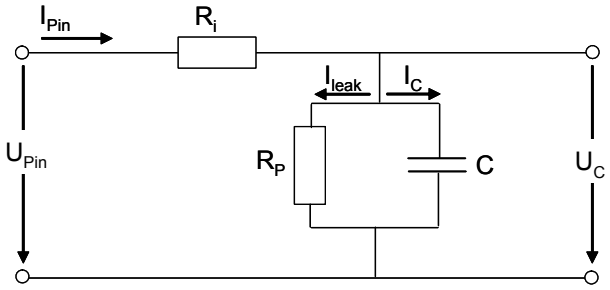

Figure 4: Equivalent electric circuit of the ultracapacitor

3.5 Internal combustion engine

The model of the internal combustion engine is a modified map-based model from the Modelica PowerTrain library. Apart from the stationary characteristic map the fuel consumption at idle speed is needed. As there is no specific data available an empirical formula is used. As a rule of thumb, a diesel engine needs in idle conditions 4mg of fuel per work cycle per 500 cm³ displacement. The engine friction is determined using a Willans curve methodology [3].

3.6 Flywheel

While the capacity of a flywheel is determined by the inertia and the maximum rotation speed of the wheel, the power is determined by the electric drive. As a result, a typical characteristic of a flywheel is shown in Figure 3. Major components of the model are a map-based electric motor and a standard Modelica inertia. Losses of the flywheel due to air friction, cooling and the vacuum pump are considered in sum as function of the rotating speed. To determinate the status of the flywheel, a state of energy is defined:

$$SoE = \frac{n^2 - n_{min}^{\ 2}}{n_{max}^{\ 2} - n_{min}^{\ 2}}$$

3.7 Ultracapacitors

The model of the ultracapacitors is an implementation of the model by van Mierlo et al in [4]. The ultracapacitor is reduced to the equivalent circuit shown in Figure 4, which can easily be modelled using standard components. Corresponding to the flywheel a state of energy is defined:

$$SoE = \frac{U_C^2 - U_{min}^2}{U_{max}^2 - U_{min}^2}$$

4 Control Strategies

The control strategy of the vehicle is divided into three layers. The first layer controls the higher-level functions of the vehicle independently from the power train components. It controls the velocity of the vehicle and communicates the desired acceleration or deceleration to the second and third control layers. The second layer manages the distribution of power and energy among the different power train and storage components. The third layer acts on the level of single components and controls their operation status depending on the desired power.

4.1 First control layer

The first control layer defines the way of driving implemented in the control strategy. The general aim of the control strategy is to achieve the shortest driving time. This means maximum acceleration until the speed limit is reached followed by a section driven with constant speed. Each change in the speed limit leads to maximum operational acceleration or deceleration. When approaching the next stop the vehicle is decelerated with the maximum operational braking force.

The first control layer uses three different states during an operational cycle. The first state is the driving state, which is used during acceleration and normal driving. In this state, the desired velocity given in the track description is controlled by a PI-Controller. When the vehicle reaches a certain distance to the next stop the state controller switches to the second state and the deceleration phase starts. This distance is dynamically calculated by means of the maximum operational deceleration and the current velocity of the vehicle. A PI-controller controls the braking signals for the power train components and, if needed, for the wheel set brakes. When the velocity reaches zero at the stopping point given in the track description the state controller switches to the third state. After a predefined stop-time the next operational cycle starts and the state controller automatically switches to the driving state.

The current state is provided to the other control systems via the signal bus of the vehicle. Therefore three Boolean signals are used which are called driving, braking and halt.

4.2 Second control layer

The second control layer determines the current electrical power of each component of the electrical drive train and storage system. In the diesel-hydraulic power train there is no choice which component has to deliver the required power. In this case the second control layer is not necessary; the power demand is transmitted directly to the controller of the internal combustion engine (DH).

In the case of the diesel-electric power train two operating strategies for the energy management are discussed. The first one (DE1) is based on the assumption that the internal combustion engine operates intermittently in its most efficient operating point [8]. If the SoE of the storage is greater 70 %, the ICE is switched off. As soon as the SoE-level falls short of 25 % the ICE is switched on again. The electrical energy is stored in the flywheel or delivered directly to the driving motors. The operation in this manner requires an energy storage with high power performance to ensure the delivery of the requested power when the ICE is stopped. On the other hand the power capability helps reducing fuel consumption due to the fact, that great amounts of braking energy can be recuperated.

The second strategy (DE2) assumes that the ICE runs permanently on a characteristic curve with low fuel consumption. In this case, the operating point of the engine depends on the current power demand of the first control layer. Whenever high power is needed, the engine runs faster and the generator demands more torque. In times of low power demand, engine speed decreases. The energy storage is primarily used to buffer braking energy; as a secondary effect it helps levelling out the engine dynamics.

4.3 Third control layer

The third control layer is implemented in each component. It controls the way how the requested power is distributed or stored, i.e. for the ICE the point or characteristic curve of operation. As this is very specific for the different components, it is not discussed any further here.

5 Simulation results

In the simulation three power train variants are compared. The first one is the model of the diesel-hydraulic (DH) power train. The others are diesel-electric power trains with identical component parameters. There is only a difference is in the control

strategy. The main parameters of the railcars are given in the table below.

	DE	DH
Vehicle mass	54.2t	51.3t
Engine power	2 x 257kW	
Flywheel usable capacity	4.5kWh	-
Flywheel max. power	500kW	-

Figure 5 shows the structure of the DE-Model with two diesel-electric generators and two electrically driven axles which are mechanically connected to the driving resistance model. The DC voltage link connects the electrical components like flywheel, braking resistance and auxiliary equipment. The controllers manage the flow of energy within the electrical and mechanical system.

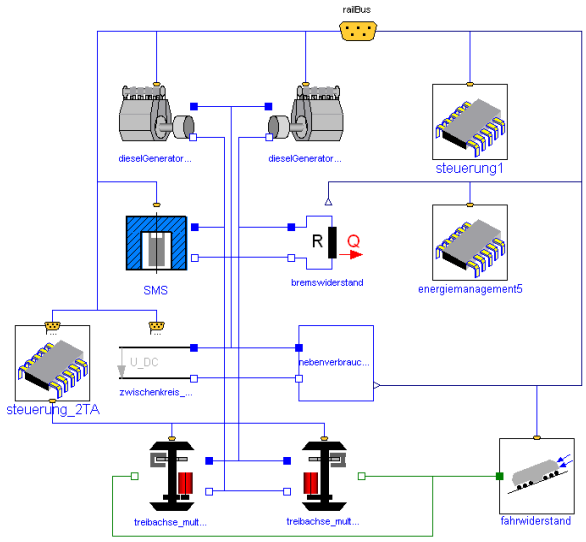

Figure 5: Model of the diesel-electric power train

The three different power train systems are simulated on a test track, which is a short sequence of a mountainous track with relatively low speed levels. The admissible maximum speed is 80km/h, the slope is up to 25‰. There are three stops within the route. Figure 6 shows the track related resistance forces for the diesel-hydraulic railcar. The rolling resistance F_Roll is almost constant, while the drag resistance F_Drag is obviously varying with vehicle velocity. The slope resistance is the most significant force and is by far the dominant resistance force on parts of the track. Compared to the other resistance forces, the force F_Curve due to the curvature of the track is relatively small. Figure 7 shows the acceleration force F_a. As the railcar travels with maximum acceleration, this force is temporarily up to ten times of the sum of the other forces.

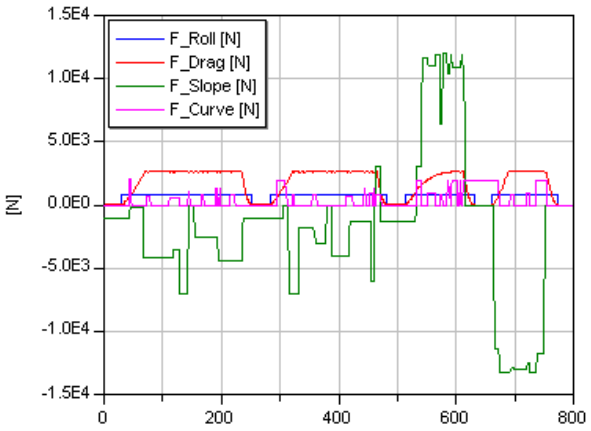

Figure 6: Resistance forces simulated with the DH-model

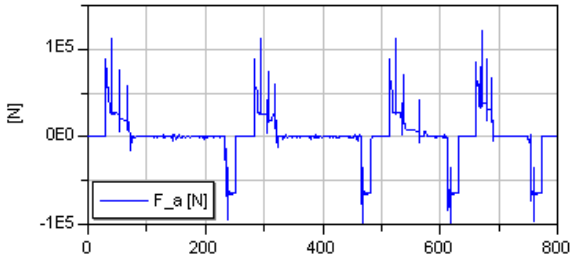

Figure 7: Acceleration force of the DH-model:

Figure 8 compares the vehicle speeds of the two diesel-electric variants and the diesel-hydraulic railcar. There are slight differences in the time needed to reach the last stop. The DH is the fastest, while the DE1-variant needs about 12 seconds longer to accomplish the track. At t = 600 s the velocity of the three variants differs significantly. Although the two DE-railcars are driven by electric motors with the same power, they don't achieve the same velocity. This is the result of the different control strategies. In the DE2 variant the power of the driving motors is limited by the controller of the energy management. This is done because the amount of energy in the flywheel is depleting even though the ICEs are running at full power. Eventually this reduction of motor power leads to the longer driving duration of this variant.

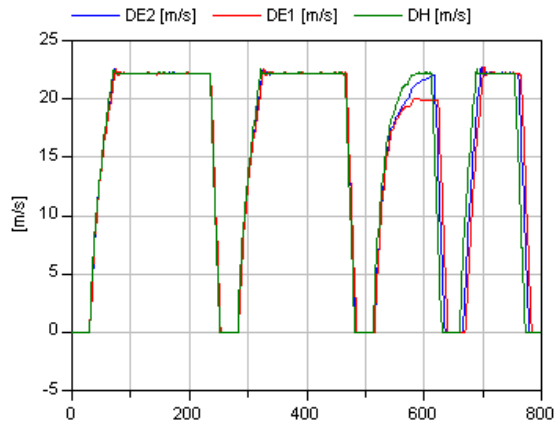

Figure 8: Comparison of the vehicle velocities

Figure 9 illustrates the state of energy SoE of the flywheel. Obviously the utilisation of the storage is much higher with the DE1-strategy. This leads to greater amounts of energy stored in and recovered from the flywheel. The capacity of the storage seems to be a good choice for the DE1 variant, while the DE2 variant does not necessarily need such a big storage. In this variant at least 25 % of the capacity is unused. While it is easily possible to determine a well-sized capacity for the DE2-variant, it is difficult to find the correct capacity of the DE1-variant. In the end, the capacity is responsible for the on/off-timing of the ICE. Especially if the ICE runs while the traction motors need power, the energy efficiency of the system rises. Instead of storing the electric energy in the flywheel with conversion losses, it is instantly used by the traction motors with higher overall efficiency. An optimisation of the storage capacity strongly depends on the driving cycle, the SoE at start and the on/off-timing of the ICE.

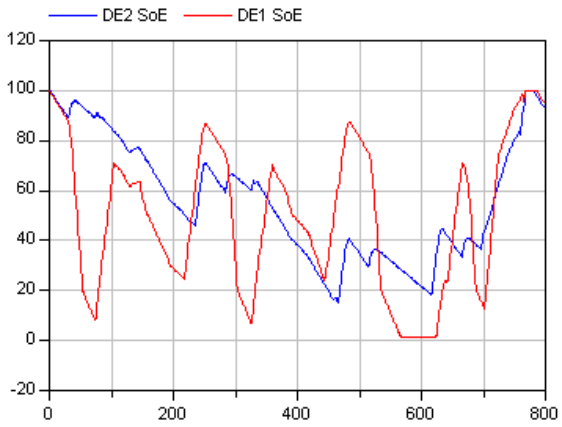

Figure 9: State of Energy of the flywheel

Differences between the DE-variants are also in the amount of power the flywheel must be capable of. Figure 10 shows the power curves for both variants.

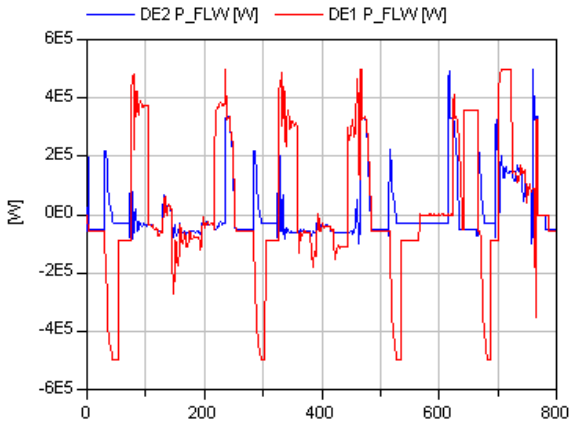

Figure 10: Power at the flywheel

While the DE1 variant needs a flywheel with power up to 500 kW, the DE2 variant could be equipped with a flywheel with less power. The DE2 strategy covers a great amount of the demanded power by the ICEs, the DE1 variant prefers the storage to cover the vehicles power requirements.

The energy flow within the electrical system of the DE-models is shown in Figure 11 and Figure 12. The energy flows of the generators and the traction motors are slightly different, but in the same dimension. The differences in the flywheels energy are remarkable. As already discussed with the state of energy curve, the DE1 variant stores plenty of energy in the flywheel. The figure shows that not only the recuperated braking energy is stored but also a great amount of the electrical energy produced by the diesel-generators.

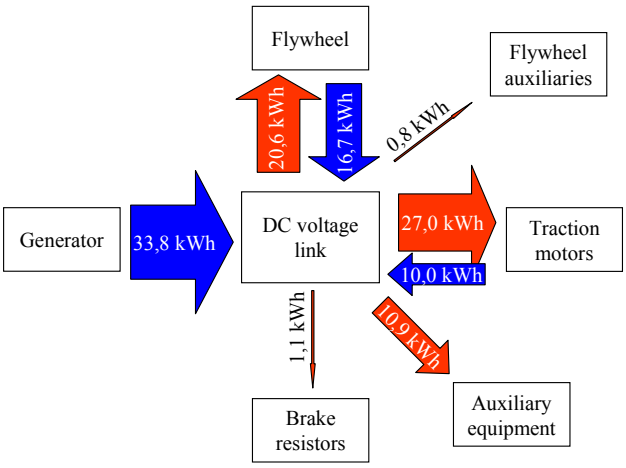

Figure 11: Electrical energy flow of DE1

The DE2 variant does not even store all the recuperated energy. Partly the braking energy is consumed by the auxiliary equipment, and some parts are transformed to heat in the brake resistors.

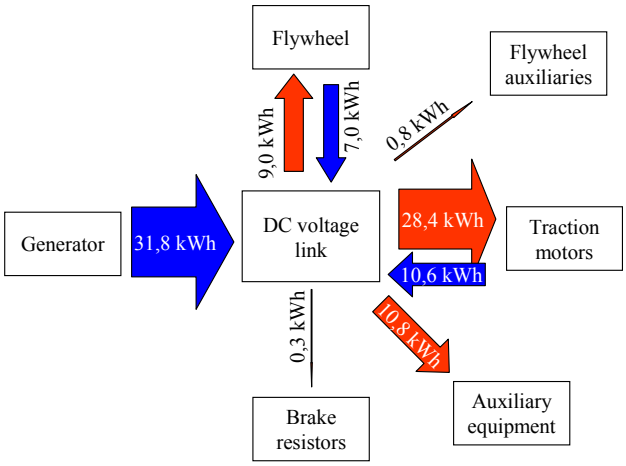

Figure 12: Electrical energy flow of DE2

The fuel consumption of the three variants is shown in Figure 13. The best energy efficiency is obtained with the diesel-electric variant DE1, which uses the intermittent control strategy for the ICE. The fuel consumptions of DE2 and DH are close together at the last stop. During driving there are partly strong differences between all strategies.

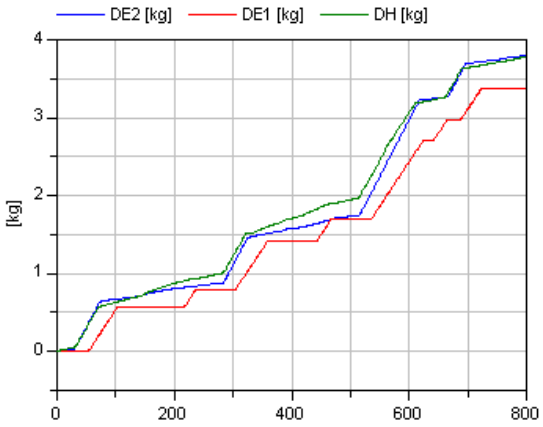

Figure 13: Fuel consumption of one diesel-engine

The comparison of the fuel consumption and the energy flows in the DC voltage link shows that DE1 consumes less fuel than DE2. This is especially remarkable because the amount of electrical energy produced by the generator is greater with DE1 than with DE2. This result proves the enhanced efficiency of the ICE as a consequence of the usage in its most efficient operating point. It has to be stated that these conclusions are specific for the chosen line characteristics and vehicle parameters. Especially the dominance of the slope resistance requires customizing the control strategy by needs of the line topology.

6 Conclusions

The model presented in this work is a starting point of hybrid railcar simulation in Modelica. It turns out, that a number of models that were primary developed for automotive simulations can be adapted to railroad vehicles. Therefore the effort to set up the simulation is moderate. The simulation gives an idea of the energy saving potential of hybrid power trains even in railroad vehicles. However the shown serial hybrid is the most simple hybrid power train, parallel or power-split hybrids should be investigated in further. As the simulations with the different control strategies demonstrated, there is a strong influence of the control strategy on the achievable fuel consumption of a predefined vehicle.

References

[1] Wende, D. Fahrdynamik des Schienenverkehrs. B.G. Teubner Verlag/GWV Fachverlage GmBH, Wiesbaden, 2003

[2] Filopovic, Z. Elektrische Bahnen. Springer Verlag, Berlin, Heidelberg, New York, 1992

[3] Kuhlmann, P. Grundlagen der Verbrennungsmotoren, lecture notes Unversität der Bundeswehr, Hamburg, 1990

[4] van Mierlo, J., van den Bossche, P., Maggetto, G. Models of energy sources for EV and HEV: fuel cells, batteries, ultracapacitors, flywheels and engine-generators. Elsevier Journal of Power Sources No. 128, 2004

[5] Wallentowitz, H. Längsdynamik von Kraftfahrzeugen Schriftenreihe Automobiltechnik Forschungsgesellschaft Kraftfahrwesen Aachen mbH, 2002

[6] Göhring, M. Betriebsstrategien für serielle Hybridantriebe Dissertation, RWTH Aachen, 1997